Supporting Information

Ionic Liquid-Assisted One-Step Preparation of Ultrafine Amorphous Metallic Hydroxide Nanoparticles for Highly Efficient Oxygen Evolution Reaction

Youhai Cao,[a,&] Song Guo,[a,&] Changlin Yu,[b] Jiangwei Zhang,[a] Xiaoli Pan,[a] Gao Li[a,c,d*]

[a] State Key Laboratory of Catalysis, Dalian Institute of Chemical Physics, Chinese Academy of Sciences, Dalian 116023, P.R. China.

[b] School of Chemical Engineering, Key Laboratory of Petrochemical Pollution Process and Control, Guangdong Province, Guangdong University of Petrochemical Technology, Maoming 525000, China

[c.] School of Chemistry and Chemical Engineering, Qufu Normal University, Qufu 273165, China.

[d] University of Chinese Academy of Sciences, Beijing 100049, China.

[&.] Y.C. and S.G. contributed equally.

Email: gaoli@dicp.ac.cn

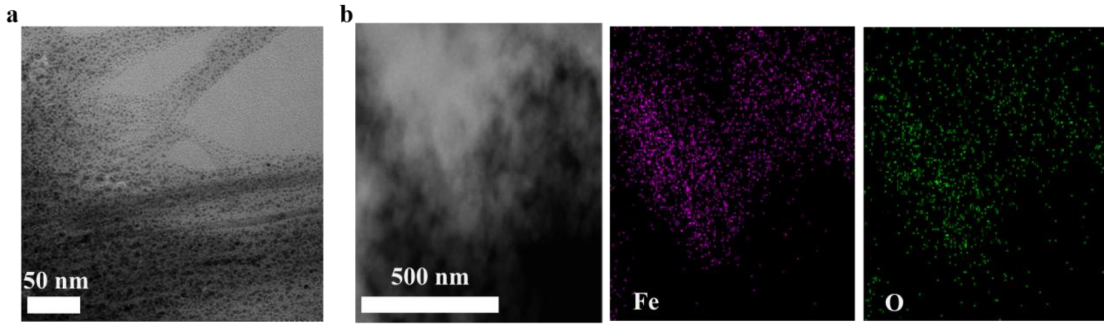

Figure S1. Fe@IL/C: (a) TEM image. (b) STEM-EDX elemental mappings of Fe and O.

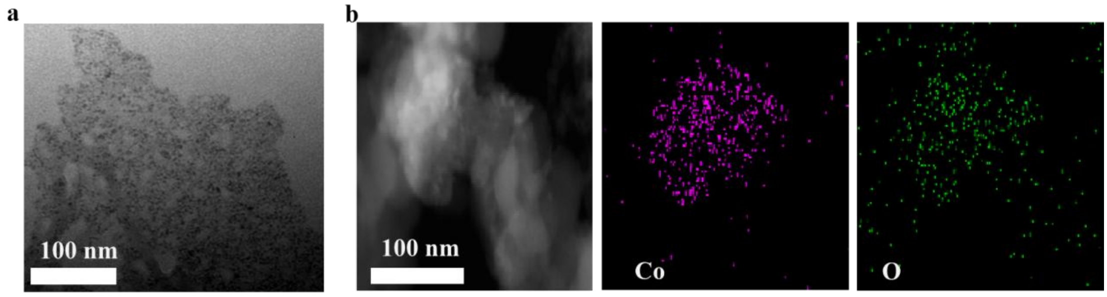

Figure S2. Co@IL/C: (a) TEM image. (b) STEM-EDX elemental mappings of Co and O.

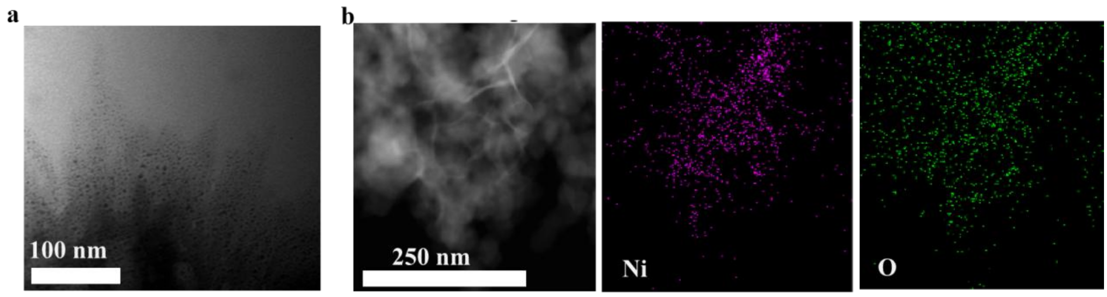

Figure S3. Ni@IL/C: (a) TEM image. (b) STEM-EDX elemental mappings of Ni and O.

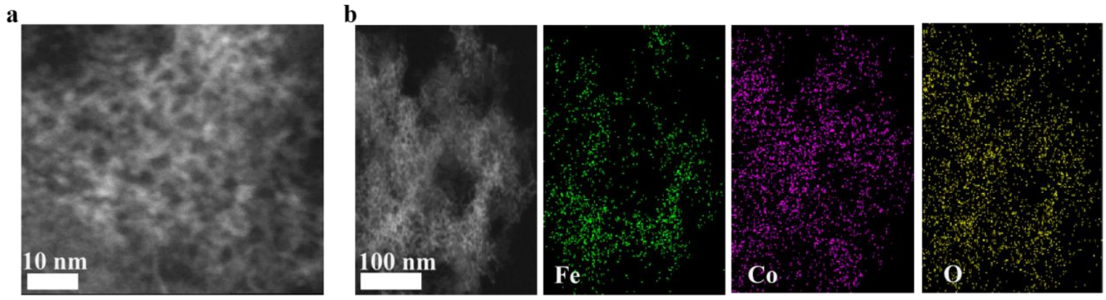

Figure S4. FeCo@IL: (a) HAADF-STEM image. (b) STEM-EDX elemental mappings of Fe, Co and O.

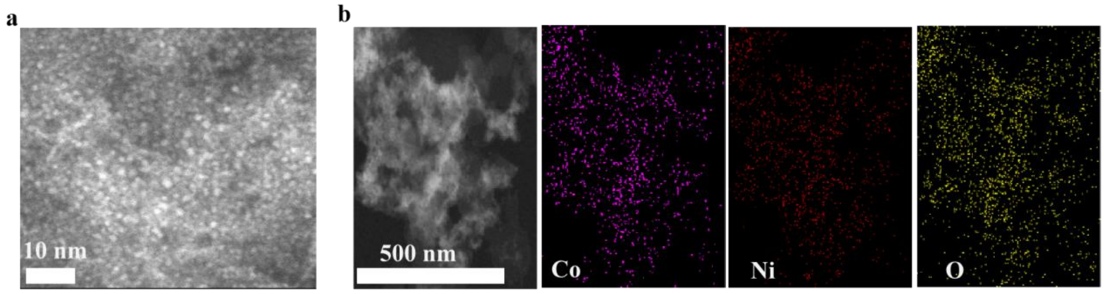

Figure S5. CoNi@IL: (a) HAADF-STEM image. (b) STEM-EDX elemental mappings of Ni, Co and O.

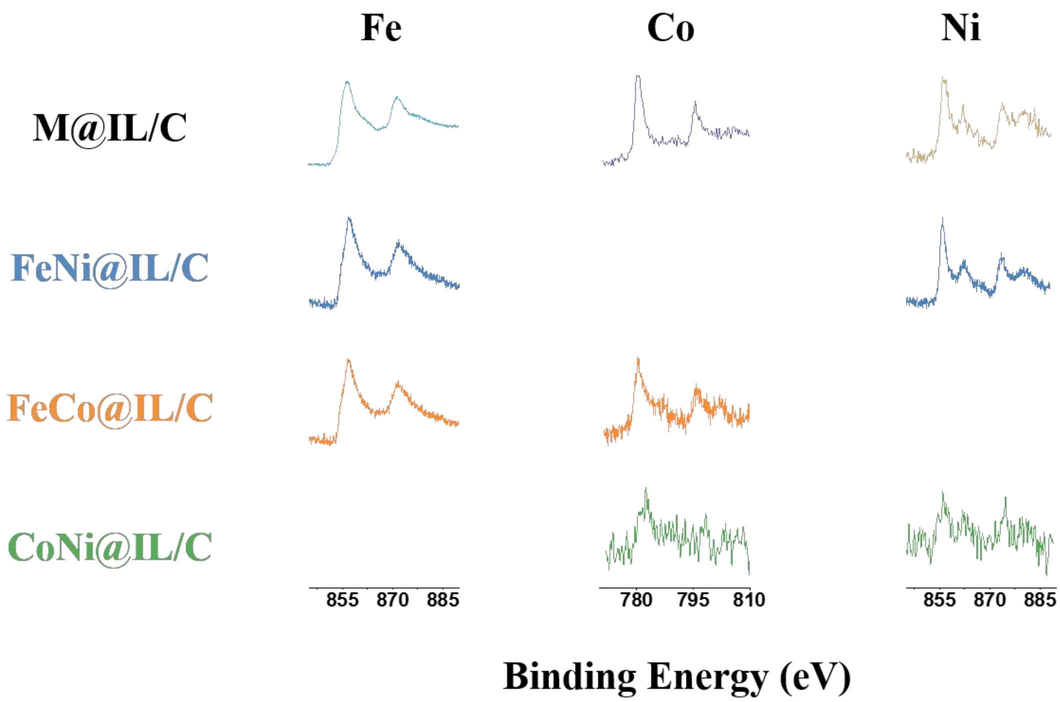

Figure S6. XPS spectra recorded on bi-metal hydroxides. Spectra for Fe@IL/C, Co@IL/C, and Ni@IL/C are provided for comparison.

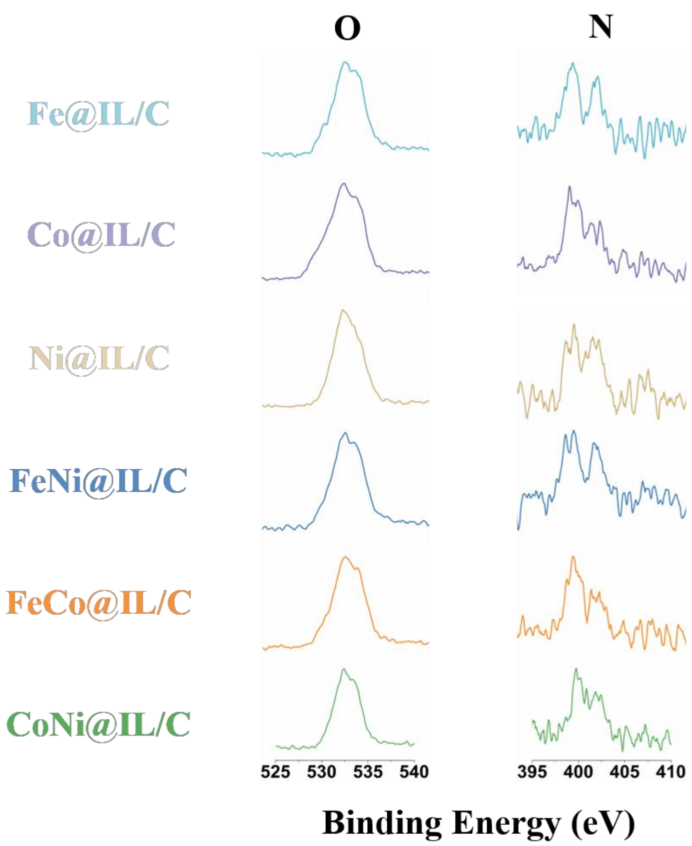

Figure S7. The O 1s and N 1s XPS spectra of M@IL/C.

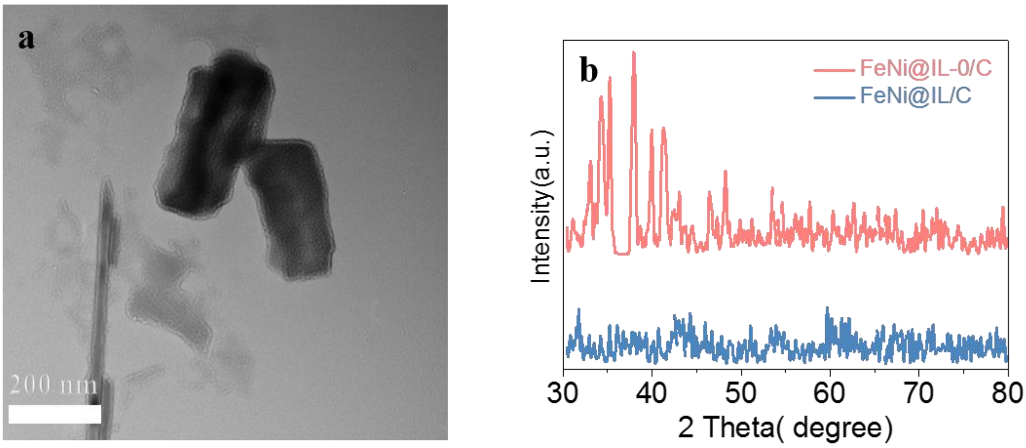

Figure S8. (a) TEM image of FeNi nanoparticles without IL. (b) The XRD spectra of FeNi@IL/C in the presence or absence of IL. The XRD peaks in FeNi@IL-0/C are assigned to crystalline phases of Fe/Ni-OH. [S1, S2]

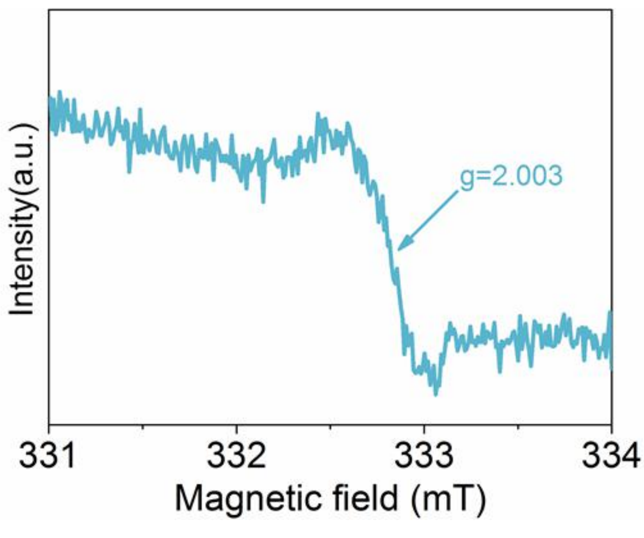

Figure S9. Electron paramagnetic resonance (EPR) curves of FeNi@IL/C.

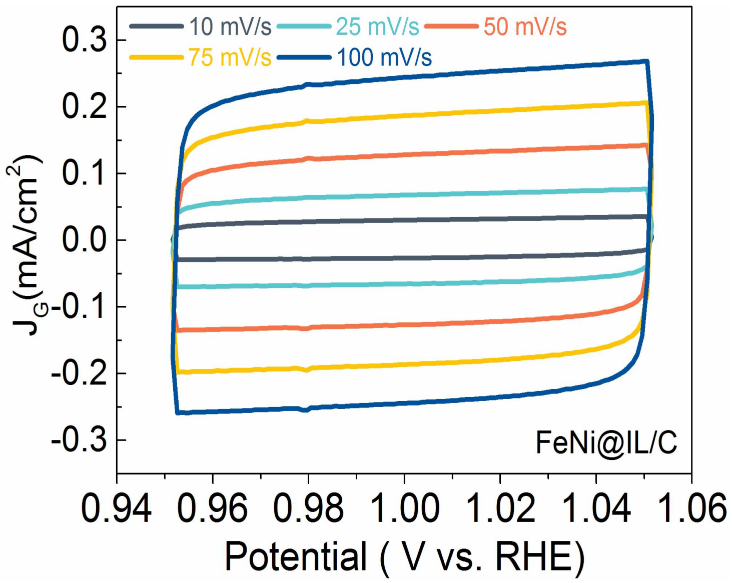

Figure S10. The CVs at different scan rates in a potential window where no Faradaic processes for FeNi@IL/C.

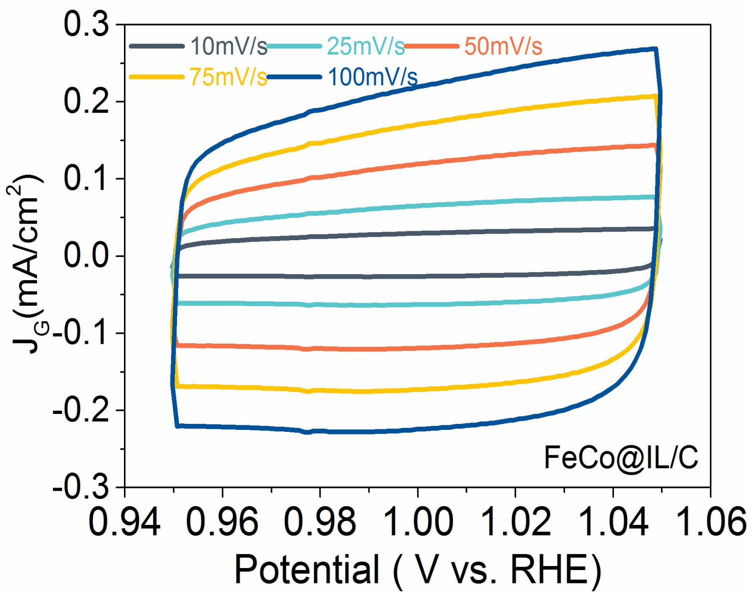

Figure S11. The CVs at different scan rates in a potential window where no Faradaic processes for FeCo@IL/C.

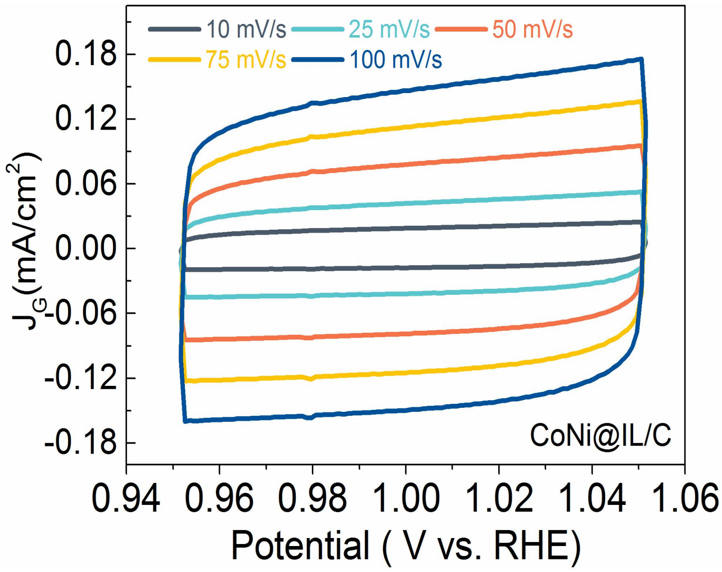

Figure S12. The CVs at different scan rates in a potential window where no Faradaic processes for FeNi@IL/C.

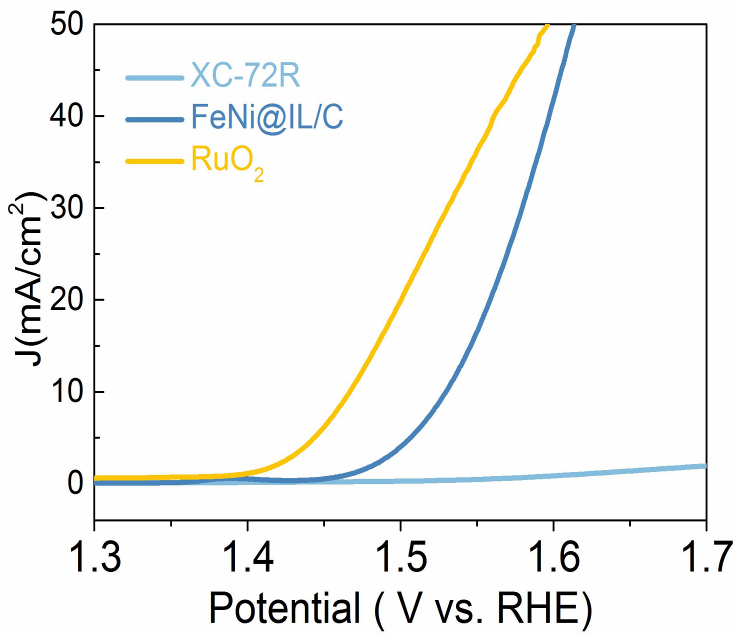

Figure S13. LSV for FeNi@IL/C in comparison with XC-72R carbon and RuO_2 with the same mass loading.

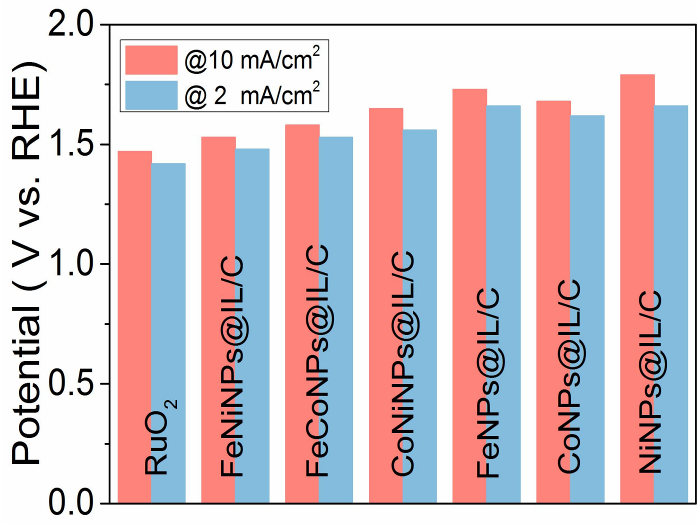

Figure S15. The potential required for FeNi@IL/C and RuO_2 at 2 mA cm^{-2} and 10 mA cm^{-2}.

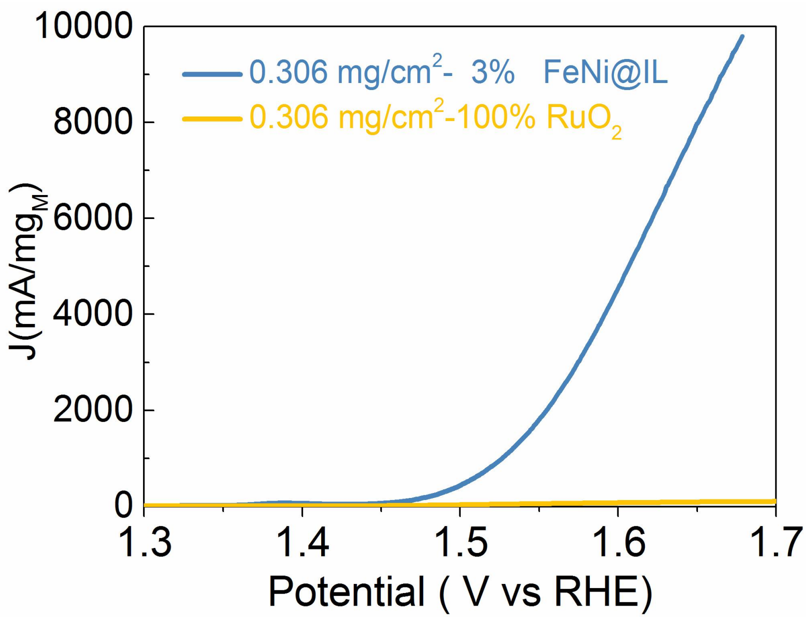

Figure S15. Mass activities of FeNi@IL/C and commercial RuO_2 for OER.

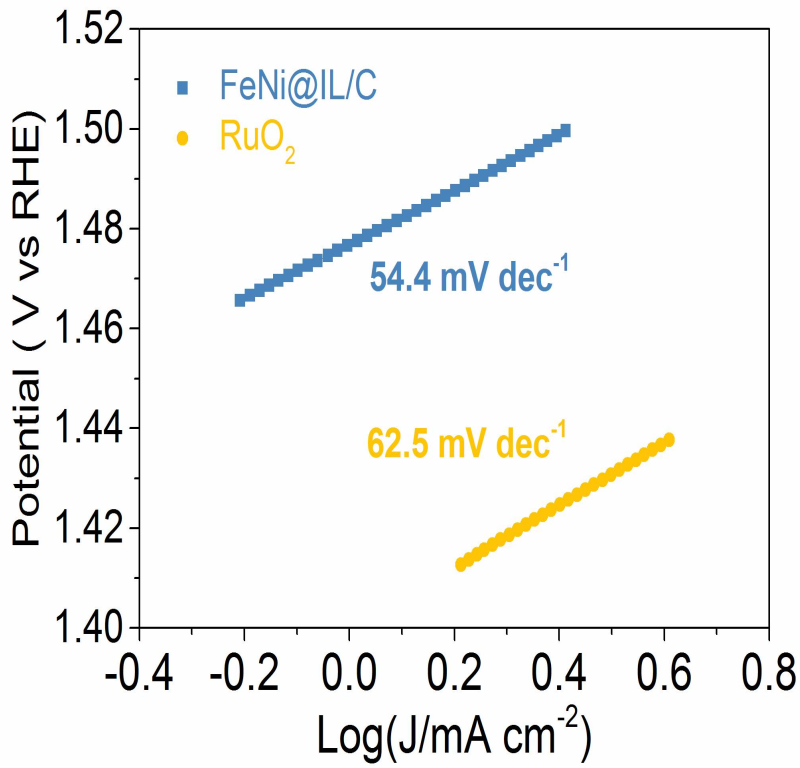

Figure S16. Tafel plots for FeNi@IL/C and RuO_2.

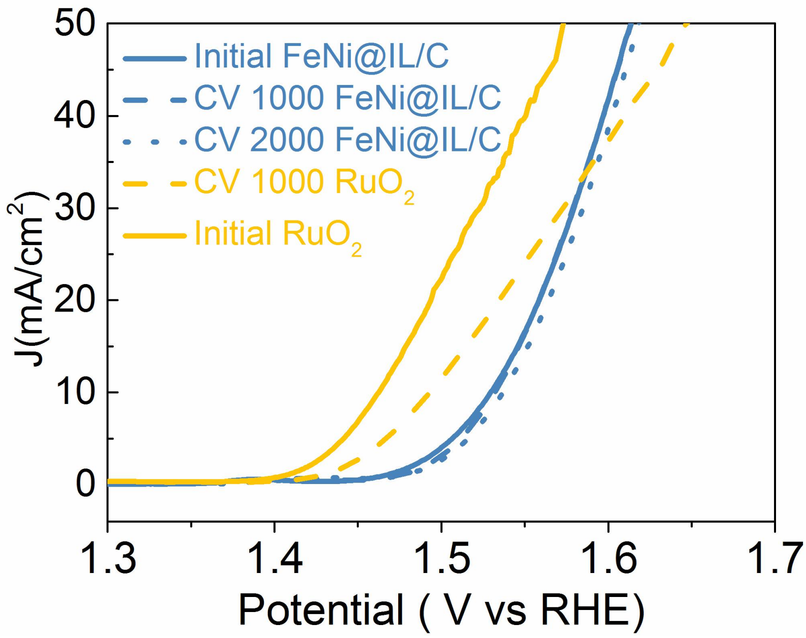

Figure S17. Durability test of FeNi@IL/C in an alkaline electrolyte in contrast to RuO_2.

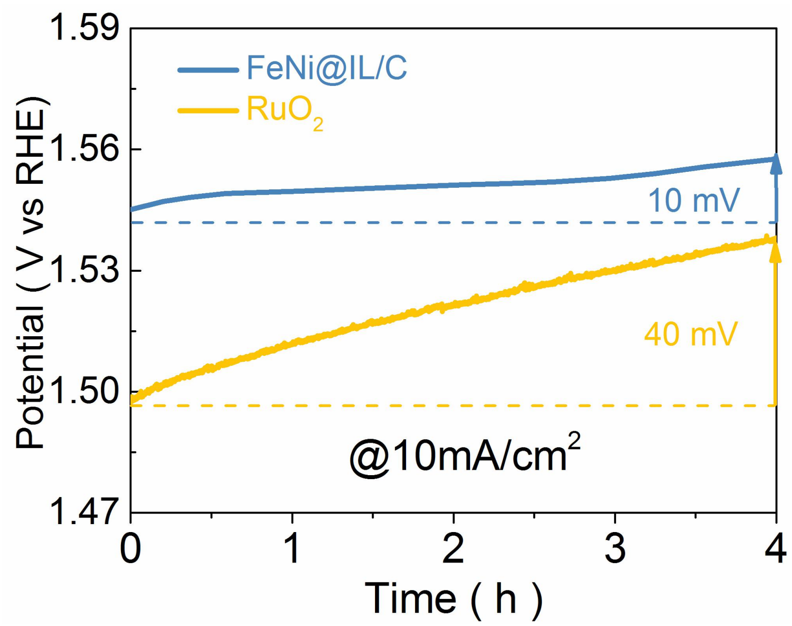

Figure S18. Chronoamperometric durability test in current densities at 10 mA cm^{-2} FeNi@IL/C and RuO_2.

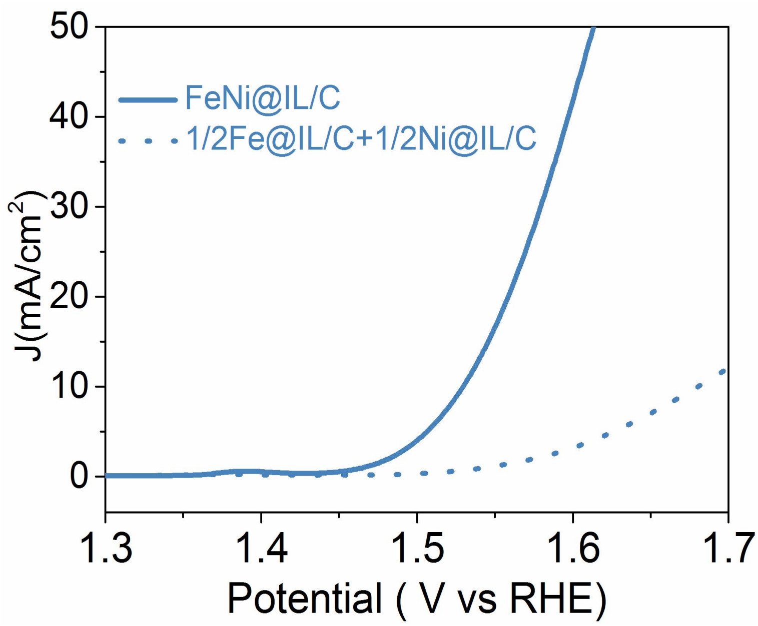

Figure S19. Comparison of the OER activity of FeNi@IL/C with the physically mixed mon-metallic catalysts of Fe@IL/C and Ni@IL/C. The total metal loadings of all catalysts were kept the same.

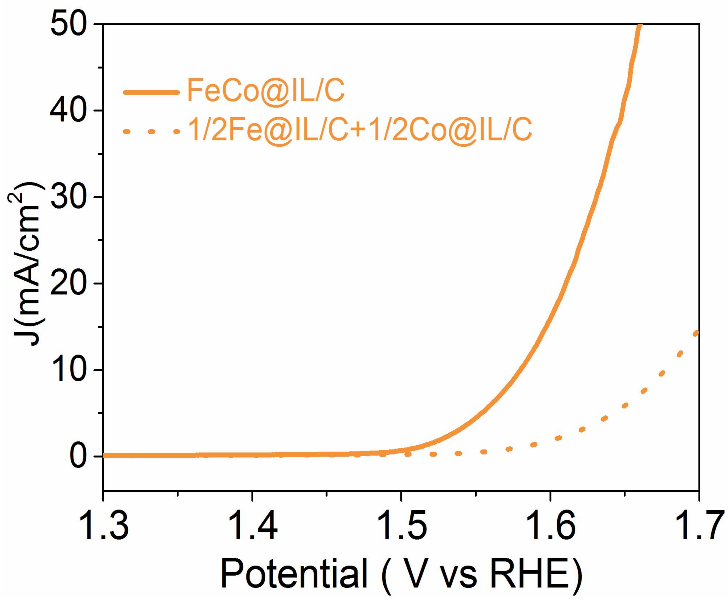

Figure S20. Comparison of the OER activity of FeCo@IL/C catalysts with physically mixed mon-metallic catalysts of Fe@IL/C and Co@IL/C. The total metal loadings of all catalysts were kept the same.

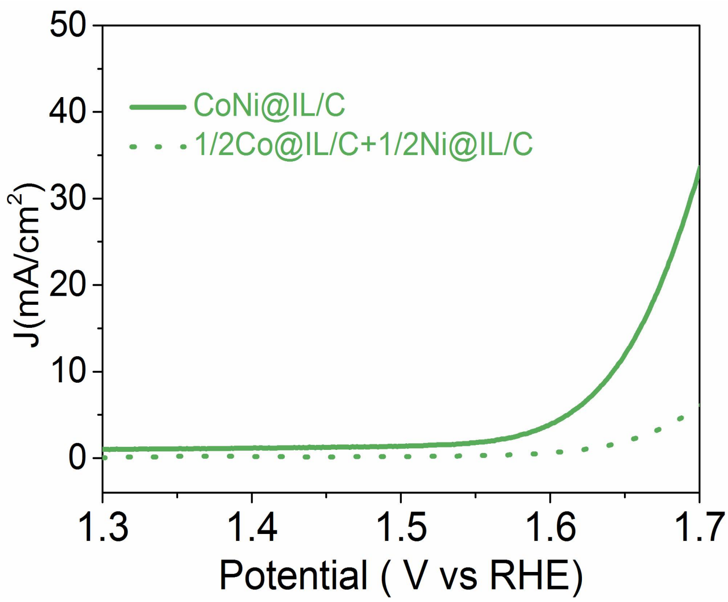

Figure S21. Comparison of the OER activity of CoNi@IL/C catalysts with physically mixed mon-metallic catalysts of Co@IL/C and Ni@IL/C. The total metal loadings of all catalysts were kept the same.

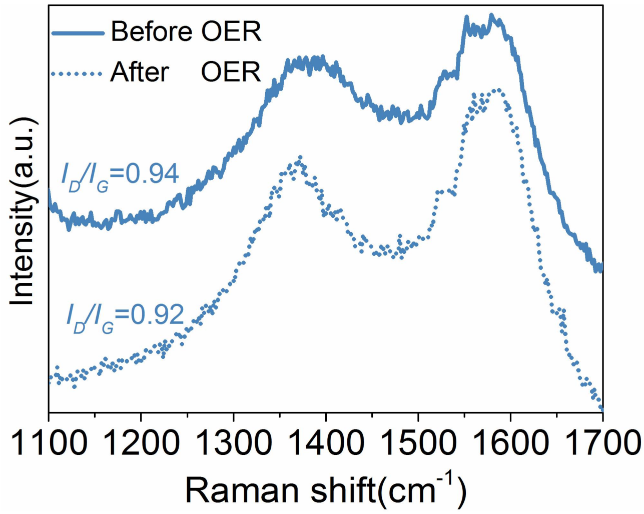

Figure S22. Raman spectra of the FeNi@IL/C catalysts before and after OER.

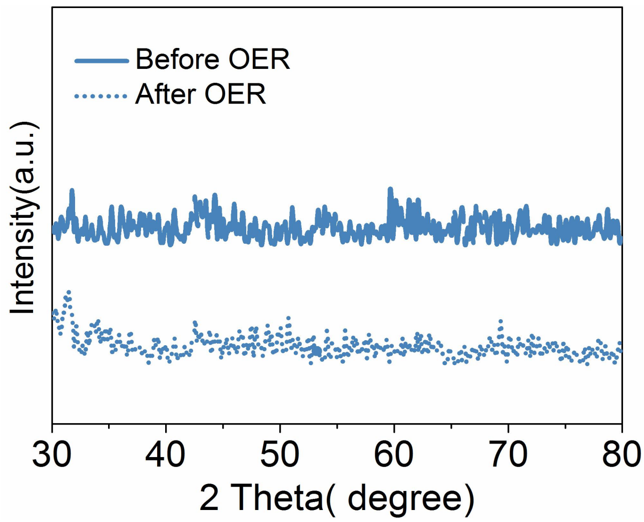

Figure S23. XRD analysis of the FeNi@IL/C catalysts before and after OER.

Table S1. Turnover frequency of various catalysts at the η=250 mV.

Catalysts	FeNi@IL/C	FeCo@IL/C	CoNi@IL/C	Commercial RuO_2
TOF (s^{-1})	0.0259	0.0061	0.0048	0.0164

Table S2. Summary of the catalytic performance of representative OER catalysts.

Catalysts	Amount (mg/cm^2)	Eletrolyte solution	Current Density	Potential (V vs. RHE)	Ref.
FeNi@IL	**0.009**	1 M KOH	10 mA/cm^2	**1.53**	This work
			10 A/g	**1.34**	
FeCo@IL			10 mA/cm^2	1.58	
CoNi@IL			10 mA/cm^2	1.65	
RuO_2	0.306	1 M KOH	10 mA/cm^2	1.47	
			10 A/g	1.46	
FeNi@NC	0.32	1 M NaOH	10 mA/cm^2	1.51	S3
IrO_2	0.32	1 M NaOH	10 mA/cm^2	1.52	S3
a-NiFe-LDH/CNT	0.20	1 M KOH	10 A/g	1.458	9
			10 mA/cm^2	1.477	9
FeNi-rGO LDH	0.25	1 M KOH	10 mA/cm^2	1.44	S4
CoNi-SAs/NC	1.4	1 M KOH	10 mA/cm^2	1.57	S5
RuO_2	/	0.1 M KOH	10 A/g	1.52	S6
IrO_2	/	0.1 M KOH	10 A/g	1.52	S6
3D Ni/NiO/NF	/	1 M KOH	100 mA/cm^2	1.61	1
Cu@CeO2 @NFC	0.2	1 M KOH	10 mA/cm^2	1.46	S7
Sandwiched NiFe/C	1.0−1.3	0.1 M KOH	10 A/g	1.47	S8
a-CoFe-OH nanosheets	/	1 M KOH	10 mA/cm^2	1.51	17
a-NiFeOH/ NiFeP/NF	/	1 M KOH	10 mA/cm^2	1.43	S1
a-$Ni_2Co(OH)_x$	0.2	1 M KOH	10 mA/cm^2	1.53	18
NiO/NiFe LDH	0.2	1 M KOH	10 mA/cm^2	1.31	S9

References

S1 H. Liang,; A. N. Gandi,; C. Xia,; M. N. Hedhili,; D. H. Anjum,; U. Schwingenschlögl and H. N. Alshareef, *ACS. Energy. Lett.,* 2017, **2,** 1035-1042.

S2 L. Trotochaud, S. L. Young, J. K. Ranney and S. W. Boettcher, *J. Am. Chem. Soc.,* 2014, **136,** 6744-6753.

S3 X. J. Cui.; P. J. Ren.; D. H. Deng.; J. Deng and X. H. Bao, *Energy. Environ. Sci.,* 2016, **9,** 123--129.

S4 X. Long, J. K. Li, S. Xiao, K. Y. Yan, Z. L. Wang, H. N. Chen and S. H. Yang, *Angew. Chem.*, *Int. Ed.,* 2014, **53,** 7584-7588.

S5 X. P. Han, X. F. Ling, D. S. Yu, D. Y. Xie, L. L. Li, S. J. Peng, C. Zhong, N. Q. Zhao, Y. D. Deng, W. B. Hu. Adv. Mater. 2019, **31,** 1905622.

S6 Koper. M. T. M, *Electroanal. Chem.* 2011, **660,** 254-260.

S7 J. L. Xia, H. Y. Zhao, B. L. Huang, L. L. Xu, M. Luo, J. W. Wang, F. Luo, Y. P. Du, C. H. Yan,

Adv. Funct. Mater., 2020, 1908367

S8 Y. Feng, H. J. Zhang, L. Fang,Y. P. Mu, and Y. Wang, *ACS Catal.,* 2016, **6,** 4477−4485.

S9 Z. W. Gao, J. Y. Liu, X. M. Chen, X. L. Zheng, J.g Mao, H. Liu, T. Ma, L. Li, W. C. Wang, and X.W. Du, *Adv. Mater.*, 2019, **31,** 1804769.